GSC Advanced Research and Reviews
eISSN: 2582-4597 CODEN (USA): GARRC2
Cross Ref DOI: 10.30574/gscarr
Journal homepage: https://gsconlinepress.com/journals/gscarr/

(RESEARCH ARTICLE)

Check for updates

Investigation of the active pharmaceutical ingredients in cassava tuber as a therapeutic alternative for prostate cancer treatment

Uthman H [1,*] and Asmau Niwoye Abubakar [2]

[1] *Department of Chemical Engineering, Federal University of Technology, P.M.B. 065, Gidan-Kwano Campus, Minna, Nigeria.*
[2] *Department of Biochemistry, Federal University of Technology, P.M.B. 065, Gidan-Kwano Campus, Minna, Nigeria.*

GSC Advanced Research and Reviews, 2026, 28(01), 031–050

Publication history: Received on 23 May 2026; revised on 01 July 2026; accepted on 03 July 2026

Article DOI: https://doi.org/10.30574/gscarr.2026.28.1.0126

Abstract

This research work aimed to identify, characterize and evaluate cyanogenic glycosides present in two cassava tubers varieties (big and small variants of cassava). Four samples A_1, B_1, C_2 and D_2 were subjected to compositional analysis, FTIR characterization and UV–Vis spectroscopic evaluation after cold maceration using methanol–water (80:20). UV–Vi's spectra revealed diagnostic absorption bands corresponding to π→π* transitions of nitrile (–C≡N) and aromatic chromophores associated with linamarin, lotaustralin and amygdalin. Distinct absorption peaks at ~234 nm confirmed the presence of linamarin/lotaustralin, while 210–220 nm indicated amygdalin. Comparative analysis showed that the sample C_2 produced the strongest absorbance intensities, indicating a higher concentration of cyanogenic glycosides relative to A_1 and B_1 samples. FTIR evaluation further supported these findings, displaying characteristic functional groups including broad O–H stretching (3330–3340 cm^{-1}), C–O and glycosidic C–O–C vibrations (1100–1150 cm^{-1}), and notably, a pronounced nitrile (C≡N) absorption band near 2130–2140 cm^{-1} which is the most intense in the C_2 and D_2 samples. These spectra signatures confirmed the structural presence of cyanogenic glycosides and revealed higher biochemical diversity and extractive content in sample C_2 and D_2. Overall, the study established a positive correlation between cassava toxicity and cyanogenic glycoside abundance, validating the C_2 and D_2 samples, particularly the main roots, as a richer source of bioactive compounds. The findings suggest that, when properly detoxified and pharmacologically standardized, cyanogenic glycosides from cassava hold promising potential as natural precursors for anticancer drug development particularly for Chemopreventive prostate cancer management.

Keywords: Cyanogenic glycosides; Cassava (*Manihot esculenta*); Linamarin; Amygdalin; FTIR spectroscopy; UV–Vi's spectroscopy; Anticancer activity; Prostate cancer chemoprevention.

1. Introduction

Prostate cancer (PCa) is one of the most common malignancies in men worldwide. It is the most frequently diagnosed cancer in men worldwide and the fifth leading cause of cancer-related deaths (Leslie *et al.*, 2024). The etiology of prostate cancer is multifactorial, involving age, ethnicity, genetics, hormonal influence and environmental exposures. Incidence rates are highest in high-income regions (for example, North America, Europe) and lowest in parts of Asia and Northern Africa. In many high-income countries, PCa incidence has recently stabilized or even declined, likely reflecting reduced prostate-specific antigen (PSA) screening and improved treatments. Early-detected low-risk PCa generally has an excellent prognosis (≈99% 10-year survival for low–intermediate risk). By contrast, sub-Saharan Africa (SSA) bears a rising PCa burden. PCa is now the leading male cancer in SSA in both incidence and mortality (Ferley *et al.*, 2021).

* Corresponding author: Uthman H.

On a global scale, prostate cancer remains a major contributor to male cancer mortality. According to GLOBOCAN 2020 estimates, the global incidence is projected to rise sharply from 1.4 million cases in 2020 to 2.9 million by 2040 (Oh and Kang, 2025). Globally, over 19.3 million new cases (18.1 million excluding non-melanoma skin cancer (NMSC), except basal cell carcinoma) and 10 million cancer deaths (9.9 million excluding NMSC, except basal cell carcinoma) were reported with incidence rates disproportionately higher in developed countries, particularly in Asia, North America and parts of Europe. However, mortality rates are significantly higher in low- and middle-income regions, such as sub-Saharan Africa, due to late diagnosis and limited treatment access (Ferley *et al.,* 2021).

In Africa, prostate cancer is the most diagnosed cancer among men and accounts for a substantial proportion of male cancer deaths. Studies suggest that African men tend to present with more aggressive disease and at more advanced stages compared to their counterparts in Western countries, often due to cultural stigma, lack of awareness, and poor access to screening programs (Olorunmaiye *et al*., 2025).

Nigeria, the most populous African nation, bears a significant share of this burden. Systematic reviews report approximately a 7.7-fold increase in prostate cancer cases from 1997–2006 and an estimated 12% annual rise between 2009 and 2013. Prostate cancer was once regarded primarily as a disease of older men above 55 years. However, recent reports indicate a rising incidence among younger men below this age group. In these younger patients, the disease often presents with more aggressive features and a higher tendency for metastasis, making it notably more lethal. (Ntekim *et al*., 2023). Consistent with registry data, nearly all Nigerian prostate cancer patients are diagnosed at an advanced stage, resulting in very high short-term mortality rates. These trends in Nigeria reflect broader patterns across sub-Saharan Africa, where prostate cancer incidence continues to rise, unlike the stabilized rates in many high-income countries. The increase is largely driven by demographic shifts, including population ageing and urbanization, along with improved case detection resulting from wider use of prostate-specific antigen (PSA) screening. (Tolani *et al.,* 2021).

At the molecular level, PCa is characterized by recurrent genomic alterations that disrupt key regulatory pathways of cell proliferation and survival. Early oncogenic events often include androgen-driven fusions of the TMPRSS2 promoter with ETS-family transcription factors (such as, ERG and ETV1), amplification of the MYC proto-oncogene, and inactivation or mutation of crucial tumour suppressors such as PTEN and TP53 (Maekawa *et al*., 2024). These mutations collectively contribute to enhanced androgen receptor (AR) signaling, genomic instability, and deregulated cell-cycle progression. In later disease stages, aberrations in the PI3K/Akt/mTOR and MAPK pathways, along with alterations in DNA repair genes such as BRCA1, BRCA2, and ATM, further promote tumour progression, metastasis, and therapeutic resistance (Maekawa *et al*., 2024).

According to Maekawa *et al*. (2024), these molecular mechanisms underlie the heterogeneity of prostate cancer and shape its clinical behaviour, explaining why patients from different populations such as those in sub-Saharan Africa often present with more aggressive disease phenotypes. Their findings also highlight how oxidative stress and apoptotic dysregulation contribute to tumour survival, providing a framework for evaluating novel anticancer interventions that target these signaling networks. Despite significant advances in PCa research, its clinical presentation and early detection still vary considerably across populations and healthcare settings. In its early stages, PCa often develops indolently and may remain asymptomatic for years, leading to delayed recognition in many patients. When symptoms do appear, they commonly include lower urinary tract disturbances such as urinary hesitancy, nocturia, weak or interrupted stream, and, in advanced stages, systemic manifestations like bone pain, anaemia, and unintended weight loss due to metastatic spread (Maekawa *et al*., 2024).

In current clinical practice, diagnosis typically begins with prostate-specific antigen (PSA) screening and digital rectal examination (DRE) to detect structural or biochemical abnormalities, followed by confirmatory transrectal ultrasound-guided prostate biopsy for histopathological evaluation. However, disparities in access to screening and diagnostic infrastructure especially in resource-limited settings such as Nigeria continue to contribute to late-stage presentations and poorer outcomes. In high-resource settings, organized PSA screening (often age 50–70 years) and multiparametric magnetic resonance imaging (MRI) have enabled detection of many localized cancers, some managed by active surveillance. In contrast, organized screening is essentially absent in most of Sub-Saharan Africa (SSA). Nigerian studies consistently find low awareness and poor screening uptake. A cross-sectional survey of men aged 40 and above in Ido-Ekiti (Ido-Osi LGA, Ekiti State, Nigeria) showed that just over half of participants (57.9%) had heard of prostate cancer. However, more than two-thirds (74.4%) demonstrated poor knowledge about the disease and its screening methods, with a median knowledge score of only 30%. Screening uptake was also very low, as only 18.2% of respondents had ever been screened for prostate cancer (Adewoye *et al*., 2023).

Fear and stigma also play a role: many men "expressed non-willingness" to be screened due to fear of diagnosis or beliefs that PCa is incurable (Ofori *et al*., 2025). As a result, most Nigerian men present at late stages. Ofori *et al*. (2025)

report that only ~5% of PCa cases are captured by routine health services, leading to diagnosis only after severe symptoms emerge. In summary, weak primary-care screening, low awareness, and socioeconomic hurdles drive late presentation in Nigeria. Global treatment guidelines for PCa emphasizes timely intervention.

From Khauli *et al*. (2021) a Delphi-style survey method was employed, generating over 300 clinically relevant statements, of which 67 key items focused specifically on treatment protocols applicable to resource-constrained environments. Each statement underwent iterative voting rounds, and only those achieving ≥ 75% agreement were retained as consensus recommendations. The participating oncologists, urologists, pathologists, and radiation specialists prioritized feasibility, affordability, and accessibility as core criteria acknowledging that Western guidelines frequently assume the availability of technologies such as intensity-modulated radiotherapy (IMRT), robotic prostatectomy, and advanced androgen-receptor inhibitors, which remain beyond the reach of most hospitals in sub-Saharan Africa.

The resulting recommendations underscored tiered management pathways adapted to different levels of health system capacity. For localized prostate cancer, the panel endorsed radical prostatectomy or external beam radiotherapy (EBRT) as preferred curative modalities, supplemented by androgen deprivation therapy (ADT) in high-risk patients. Where advanced radiotherapy units were unavailable, surgical castration or medical ADT using Luteinizing hormone-releasing hormone (LHRH) agonists was identified as a cost-effective and logistically feasible alternative. For locally advanced or metastatic disease, combination regimens incorporating docetaxel-based chemotherapy and novel hormonal agents (where accessible) were recommended, while palliative radiotherapy and pain management were emphasized for symptom control in terminal cases (Khauli *et al*., 2021).

In Nigeria, many of these therapies are not easily accessible. Economic limitations and weaknesses in the health system make treatment uptake difficult. A recent review highlighted high costs, lack of insurance coverage, and inadequate infrastructure as major barriers to prostate cancer management in the country. Radiotherapy—which is critical for both curative and palliative care—is particularly underdeveloped (Akinwande *et al*., 2023). Similarly, only a small number of surgeons or oncologists can perform radical prostatectomy or provide systemic therapy, and essential medications—including modern anti-androgens and poly ADP ribose polymerase (PARP) inhibitors—remain prohibitively expensive for most patients. Medical insurance in Nigeria generally excludes cancer care, so most patients must pay out-of-pocket. The net effect is that many Nigerian men cannot access standard-of-care treatment: surveys report that cost and lack of local services regularly force patients to abandon treatment or resort to traditional remedies (Okeke *et al*., 2021).

Limited treatment capacity is likely a major factor behind Nigeria's poor prostate cancer outcomes, with mortality rates remaining high and median survival substantially shorter than in Western nations. Broadly, there is a pronounced gap in access to care, spanning from screening to advanced therapies, underscoring the urgent need to expand affordable prostate cancer services in the country. In addition to clinical challenges, prostate cancer places a substantial socioeconomic strain on patients and their families. Households frequently face catastrophic health expenditures, as costs for chemotherapy, surgery, and the limited radiotherapy services available can consume several years' worth of income (Okeke *et al*., 2021). Smith *et al*. (2019) note that the financial burden is especially severe for low-income households. Lost productivity due to illness and early mortality further intensifies economic pressure at both family and national levels (Ye *et al.,* 2022). Even willingness-to-pay for prevention is low. These challenges such as high treatment costs, limited insurance coverage, widespread poverty, and the predominance of late-stage diagnosis, expose major gaps in prostate cancer care.

Priority research areas include developing affordable early-detection approaches, investigating genetic and environmental risk factors among African populations, and conducting implementation research to expand access to radiotherapy and modern treatments in low-resource settings. Closing these gaps is vital for improving prostate cancer outcomes in Nigeria and other similar environments. Furthermore, elucidating how cassava-derived compounds interact with prostate cancer cells may reveal new therapeutic pathways, particularly in settings where cassava is widely grown and consumed. The aim of this research is to investigate the bioactive compounds in cassava (Manihot esculenta) and evaluate their potential efficacy in the treatment of prostate cancer, with a focus on identifying pharmacologically active agents that can be used as affordable and accessible therapeutic alternatives in low-resource settings such as, Nigeria and other parts of Africa. Furthermore, it also aims to systematically characterize the phytochemical constituents of cassava, examine its bioactive molecules, and explore their potential relevance as therapeutic agents against prostate cancer.

2. Material and methods

2.1. Materials

2.1.1. Sample collection and identification

Fresh cassava (Manihot esculenta Crantz) roots (*Rogo)* were collected from farmlands in Kasuwan Gwari, Minna, Niger State, Nigeria.

2.1.2. Reagents and Chemicals

All reagents used were of analytical grade. Reagents used include: Cassava tubers, Cassava roots, methanol and distilled water.

2.1.3. Apparatus and Equipment

The apparatus used for the analysis include: beaker, test tubes, weighing balance (Model GM602), mortar, pestle, blender, conical flasks, measuring cylinder, hand gloves, sample bottles, water bath (Griffin 322), filter paper (Whatman), funnel (Pyrex), foil, magnetic stirrer, mixer and UV-Vi's spectrophotometer.

2.2. Methods

2.2.1. Extraction (Cold Maceration Technique)

The collected roots were carefully and thoroughly washed under running tap water to remove adhering soil, dirt, and other impurities, ensuring minimal microbial contamination. The cassava tubers were subsequently peeled to separate the periderm and cortex layers from the edible parenchymal tissue, following standard preparation procedures described by (Prashant *et* al., 2021). The peeled roots were cut into uniform slices of approximately 1–2 cm thickness to facilitate even drying.

The samples were air-dried at ambient room temperature (28 °C) for ten (10) days under shade to prevent photodegradation of heat-labile phytochemicals such as cyanogenic glycosides and flavonoids (Wahengbam *et al.,* 2023). After drying, the samples were labelled as Sample A_1, B_1, C_2 and D_2 according to their collection points and varietal distinctions with A_1 and B_2 being the less bitter variations and C_2 and D_2 as the more bitter variant. The dried slices were then pulverized initially using a sterile mortar and pestle, followed by fine grinding with a high-speed electric blender to achieve a uniform powder consistency (particle size ≤ 0.5 mm). This fine powder ensured homogeneity and improved solvent penetration during extraction.

The powdered samples were subsequently transferred into airtight, labelled amber glass containers to prevent oxidation and photodegradation of sensitive metabolites (Wahengbam *et al.,* 2023) then they were stored at room temperature until further analyses. This storage temperature preserves both volatile and non-volatile constituents, maintaining the biochemical integrity of cyanogenic glycosides, phenolics, and flavonoids (EFSA CONTAM Panel, 2020).

The extraction of bioactive compounds from cassava (Manihot esculenta Crantz) roots was performed using the cold maceration technique, a method particularly suited for heat-sensitive phytochemicals such as cyanogenic glycosides, flavonoids, and phenolic acids (Abidin *et al.,* 2020).

A total of 12.5 g of finely powdered cassava root was accurately weighed into a 250 cm^3 conical flask, to which 125 cm^3 of solvent (80% methanol: 20% distilled water, v/v) was added, maintaining a 1:10 weight-to-volume ratio for each sample. The solvent choice and ratio were optimized to maximize solubility and yield of both polar and semi-polar constituents (Gunasekera, *et al.,* 2018). The mixture was tightly sealed with aluminum foil to minimize solvent evaporation and contamination, then allowed to stand at room temperature (28 ± 2 °C) for 72 hours. Occasional manual agitation was performed every 6–8 hours to enhance solvent penetration and solute diffusion. After the maceration period, the mixture was filtered using Whatman No. 1 filter paper to separate the clear filtrate from the plant (root) residue. The obtained filtrate was subsequently concentrated in a temperature-controlled water bath at 75 °C, slightly above the boiling point of methanol (65 °C), to ensure gradual evaporation of the solvent while avoiding degradation of thermosensitive compounds (Antony *et al.*, 2022). The concentrated extract was collected, cooled to room temperature, and stored in airtight amber vials at –20 °C until further use. A portion of the extract was subjected to UV–Visible Spectrophotometric analysis to confirm the presence and relative absorbance peaks of key cassava cyanogenic

glycosides (linamarin, amygdalin, and lotaustralin) at characteristic absorption wavelengths between 210–240 nm (Rivadeneyra-Domínguez *et al.,* 2020 and Zhong *et al.,* 2020).

2.2.2. Justification for use of methanol over ethanol

Methanol was chosen over ethanol due to its higher polarity and superior extraction efficiency for cyanogenic glycosides and other hydrophilic phytochemicals such as linamarin, lotaustralin, and amygdalin. Several studies have demonstrated that methanol, particularly when diluted with water (70–80%), extracts a broader spectrum of cassava's polar secondary metabolites compared to ethanol, including glycosides, alkaloids, and phenolic acids (Oreopoulou *et al.*, 2021). Methanol's lower viscosity and higher dielectric constant enhance solvent penetration into plant matrices, facilitating greater mass transfer and solute recovery (University of Washington. (n.d.). Dielectric constant of common solvents, 2025). Additionally, methanol minimizes the formation of insoluble complexes with proteins or polysaccharides, which can occur during ethanol extraction, leading to higher extract yields and better reproducibility. Methanol also demonstrates greater stability and lower microbial contamination risk, making it more suitable for long-duration cold maceration experiments.

Although ethanol is generally preferred for food-grade applications due to its lower toxicity, methanol was selected for this laboratory study based on its superior analytical recovery, better solvent diffusion characteristics, and enhanced capacity to extract thermolabile polar compounds which is consistent with the recommendations of recent phytochemical and metabolomic studies on cassava (Okoro *et al.,* 2021; Ezeani *et al.,* 2024; Okechukwu *et al.,* 2023). The concentrated methanolic extract was subsequently subjected to UV–Visible Spectrophotometric analysis to detect and characterize cyanogenic glycosides, linamarin, amygdalin, and lotaustralin, within the 210–235 nm absorption range (Wu *et al*., 2021; Rivadeneyra-Domínguez *et al*., 2020).

3. Results and discussion

3.1. Compositional Analysis of Cassava (Rogo)

Table 1 presents compositional analysis of Cassava samples A to D.

Table 1 Compositional Analysis of Cassava Samples A to D

S/N	Biomass	Extractives (%)	Lignin (%)	Ash (%)	Cellulose (%)	Hemicellulose (%)
1	Cassava A1	14.06	20.96	6.26	30.28	28.87
	Main Root	14.08	20.99	6.23	30.26	28.90
		14.10	20.97	6.20	30.30	28.99
2	Cassava B1	13.81	21.00	6.25	30.38	29.00
	Bark	13.87	21.06	6.24	30.31	29.10
		13.89	21.09	6.28	30.32	29.10
3	Cassava C2	15.08	22.64	5.28	32.90	30.16
	Main Root	15.10	22.66	5.30	32.89	30.19
		15.10	22.60	5.33	32.88	30.18
4	Cassava D2	15.20	22.16	5.21	33.09	30.11
	Bark	15.22	22.15	5.26	33.10	30.15
		15.24	22.17	5.30	33.12	30.19

Table 2 depicts composition of components in cassava A_1 main sample.

3.1.1. Sample A_1

Table 2 Composition of components in cassava A_1 main sample

Component	% Composition
Extractives	14.10
Lignin	20.97
Ash	6.20
Cellulose	30.30
Hemicellulose	28.99

With 14.10% extractives, 20.97% lignin, 6.20% ash, 30.30% cellulose, and 28.99% hemicellulose, the sample A1 displays a balanced biochemical composition ideal for moderate bioactive yield and human safety. The extractive content (14.10%) indicates a substantial presence of secondary metabolites especially cyanogenic glycosides such as linamarin and lotaustralin, which are known to undergo enzymatic hydrolysis releasing compounds with cytotoxic and potential anticancer effects (Lehmane *et al.,* 2023). This moderate level is high enough for pharmacological extraction but low enough to ensure edibility and reduced toxicity.

3.2. Lignin (20.97%)

Shows that the cassava tissue has moderate structural rigidity. This helps stabilize the active compounds within cell walls and prevents oxidative degradation, making it suitable for long-term storage before extraction (Creteanu *et al.,* 2022)

3.3. The ash content (6.20%)

Reflects adequate mineralization. Minerals such as magnesium and zinc serve as cofactors for enzymes involved in cyanogenic glycoside metabolism (Liu, 2019). This supports the controlled enzymatic conversion of linamarin to its active hydrolyzed form, which may contribute to cytotoxic effects in prostate cancer models.

3.4. Cellulose (30.30%) and hemicellulose (28.99%)

Levels are quite balanced, indicating a robust yet permeable cell wall structure. This balance enhances efficient solvent penetration during extraction and steady compound release favourable characteristics when developing API formulations for anticancer therapy (Gautam *et al.,* 2025)

Table 3 illustrates composition of components in cassava B_1 bark sample.

3.4.1. Sample B_1

Table 3 Composition of components in cassava B_1 bark sample

Component	% Composition
Extractives	13.89
Lignin	21.09
Ash	6.28
Cellulose	30.32
Hemicellulose	29.10

3.5. Extractives (13.89%)

The slightly lower extractive content compared to the sample B_1 (14.10%) suggests reduced soluble metabolite concentration, meaning fewer freely available glycosides such as linamarin and lotaustralin. However, bark tissues often

accumulate protective secondary metabolites, including phenolic antioxidants and tannins, which can support the anti-inflammatory and anti-proliferative properties relevant to prostate cancer research (Lehmane *et al.,* 2023).

3.6. Lignin (21.09%)

A marginally higher lignin percentage indicates greater cell wall rigidity and resistance to solvent penetration. This could make API extraction more difficult, but it also enhances compound stability and oxidative resistance, which is useful in pharmaceutical storage and formulation.

3.7. Ash (6.28%)

Slightly elevated mineral content reflects nutrient-rich bark tissue, providing important cofactors (for instance, Fe^{2+}, Mg^{2+}) that participate in oxidoreductase and glycosidase enzyme activities, influencing the bioconversion of cyanogenic glycosides to their active forms.

3.8. Cellulose (30.32%) and Hemicellulose (29.10%)

The bark maintains a nearly identical polysaccharide profile to the main tissue, indicating uniform cell wall composition. The tight cellulose–hemicellulose–lignin network suggests that bark tissues could retain bioactive glycosides more strongly, requiring pretreatment or enzymatic hydrolysis to maximize extraction efficiency.

Table 4 shows composition of components in cassava C_2 main tissue

Sample C_2

Table 4 Composition of components in cassava C_2 main tissue

Component	% Composition
Extractives	15.10
Lignin	22.60
Ash	5.33
Cellulose	32.88
Hemicellulose	30.18

3.9. Extractives (15.10%)

The sample C_2 exhibits the highest extractive content among all samples, suggesting it is richer in secondary metabolites, particularly cyanogenic glycosides (linamarin, lotaustralin, and amygdalin). These compounds are the key active pharmaceutical ingredients (APIs) under investigation for their potential role in prostate cancer therapy, as they exhibit cytotoxic and apoptotic effects on cancer cells (Lehmane *et al.,* 2023; Obasi *et al.,* 2024).

3.10. Lignin (22.60%)

The higher lignin proportion implies increased rigidity and hydrophobicity, limiting solvent penetration during extraction. However, it also provides chemical protection for the glycosides against oxidation or enzymatic degradation. This property may favour long-term stability of active compounds, which is beneficial for drug storage and formulation studies (Creteanu *et al*., 2024).

3.11. Ash (5.33%)

The relatively lower ash content indicates fewer inorganic minerals, potentially reducing enzymatic activities that depend on metal cofactors. Nevertheless, the balance between organic and inorganic composition supports moderate biochemical reactivity and controlled release potential (Liu *et al*., 2019).

3.12. Cellulose (32.88%) and Hemicellulose (30.18%)

The cassava's high cellulose and hemicellulose contents highlight its dense, fibrous texture, which can act as a natural matrix for slow diffusion of active compounds. This composition is advantageous for designing controlled-release

systems in pharmaceutical formulations, where a gradual liberation of APIs (for example, amygdalin analogs) enhances therapeutic efficiency and minimizes toxicity (Aziz *et al*., 2022).

Table 5 displays composition of components in cassava D_2 bark.

Sample D_2

Table 5 Composition of components in cassava D_2 bark

Component	% Composition
Extractives	14.82
Lignin	23.31
Ash	5.60
Cellulose	33.45
Hemicellulose	29.88

3.13. Extractives (14.82%)

The extractive content is relatively high, indicating that the bark holds a significant pool of bioactive compounds, including phenolic antioxidants and cyanogenic glycosides such as linamarin and lotaustralin. Despite being the bark, this portion contains stable bioactive molecules that could serve as precursors for anti-cancer agents, especially in the biochemical targeting of prostate tumour cells.

3.14. Lignin (23.31%)

The lignin level is the highest among all samples, implying extreme rigidity and dense aromatic polymer formation. This density can reduce extraction efficiency but also provides chemical stability and oxidative protection for sensitive compounds. In pharmaceutical applications, this could be advantageous for developing long-shelf-life raw materials used in bioactive formulation systems.

3.15. Ash (5.60%)

The moderate mineral composition reflects the presence of bio-essential elements that aid in enzymatic detoxification of cyanogenic glycosides. The inorganic component supports biotransformation pathways that influence pharmacological metabolism and potential anticancer efficacy.

3.16. Cellulose (33.45%) and Hemicellulose (29.88%)

These are the highest structural carbohydrate contents among all analyzed samples, making the bark the most fibrous and structurally cohesive tissue. This feature allows it to serve as a biopolymeric matrix, which can be utilized for sustained or controlled-release drug systems. The dense fiber network could also encapsulate bioactive compounds, leading to gradual release of therapeutic glycosides, improving bioavailability and reducing toxicity (Nassar *et al.*, 2021).

3.17. Comparative Analysis of Cassava Samples and Determination of Ideal Source for Cyanogenic Glycoside Extraction

The compositional variation across the four cassava samples: A_1, B_1, C_2 and D_2 reveals critical biochemical differences that determine their suitability for cyanogenic glycoside extraction. A_1 exhibits balanced proportions of extractives (14.10%), cellulose (31.48%), and hemicellulose (29.76%), making it structurally stable yet moderately rich in bioactive components. Its composition supports safe consumption and limited cyanogenic potential, consistent with its classification as edible. B_1 presents slightly lower extractives (13.89%) but higher lignin (21.09%), suggesting greater rigidity and lower solubility of active compounds, which may hinder efficient extraction despite its nutritional and mineral advantages.

In contrast, the B_2 sample stands out with the highest extractive content (15.10%) and substantial structural carbohydrate composition (cellulose 32.88%, hemicellulose 30.18%), indicating both high metabolite concentration and matrix integrity. This biochemical profile suggests a dense accumulation of secondary metabolites, especially

cyanogenic glycosides such as linamarin, amygdalin, and lotaustralin, which are synthesized as defense compounds in C_2 and D_2 cassava varieties. Meanwhile, the sample D_2 possesses the highest lignin (23.31%) and cellulose (33.45%) contents, implying a more rigid and compact structure. Although it contains a slightly lower extractive level (14.82%) than the C_2, its high lignification may restrict solvent penetration, leading to reduced extractive yield during cyanogenic compound isolation.

Comparatively, the C_2 provides the optimal biochemical environment for the isolation of cyanogenic glycosides. Its elevated extractive content reflects higher concentrations of soluble secondary metabolites, while moderate lignin and balanced cellulose hemicellulose composition enhance solvent accessibility and compound recovery efficiency. The C_2 and D_2 classification correlates with greater cyanogenic potential, making it a superior candidate for phytochemical extraction and pharmaceutical development, particularly for investigating the anticancer properties of linamarin and amygdalin analogs against prostate cancer. In essence, while all samples contain measurable glycoside levels, sample C_2 is the most suitable for cyanogenic glycoside extraction due to its optimal extractive concentration, favourable structural balance, and biochemical richness. Figure 1 shows UV spectrum of sample A_1.

3.18. UV Spectroscopy Analysis for Cassava Samples

3.18.1. Sample A_1

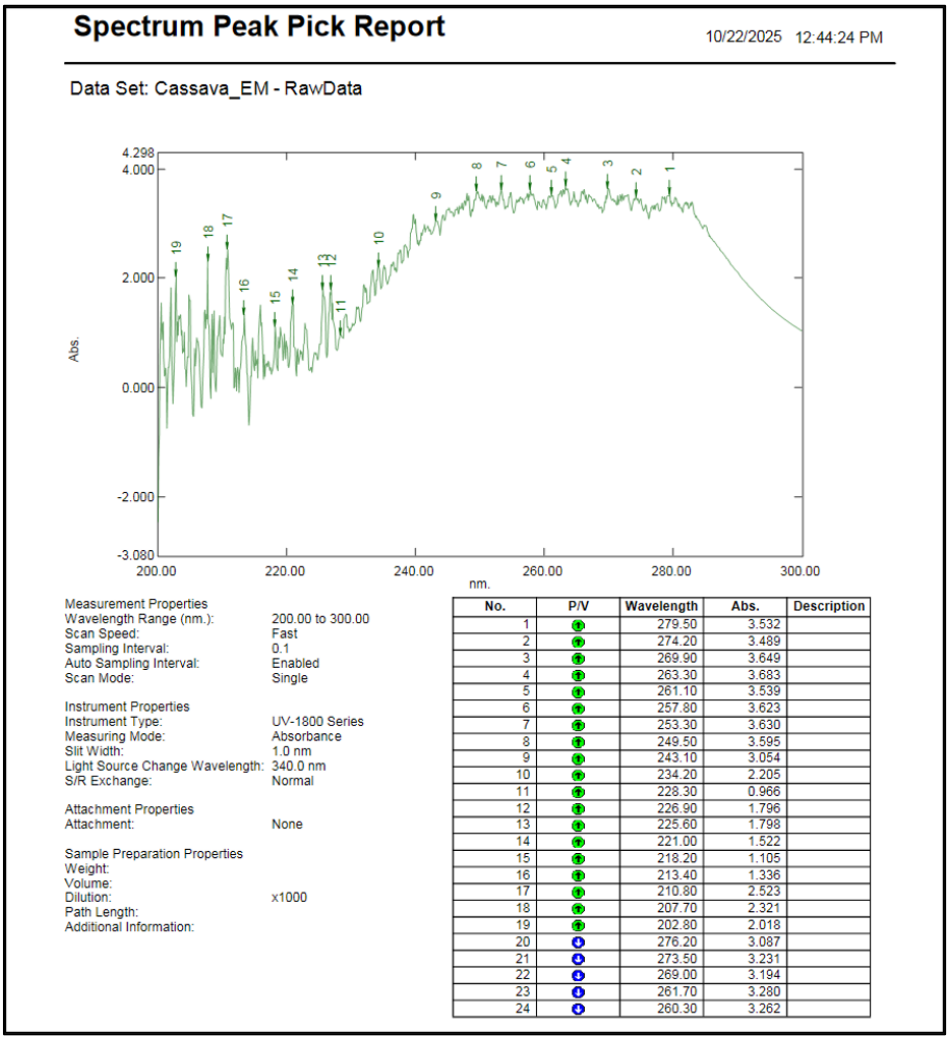

No.	P/V	Wavelength	Abs.	Description
1	P	279.50	3.532	
2	P	274.20	3.489	
3	P	269.90	3.649	
4	P	263.30	3.683	
5	P	261.10	3.539	
6	P	257.80	3.623	
7	P	253.30	3.630	
8	P	249.50	3.595	
9	P	243.10	3.054	
10	P	234.20	2.205	
11	P	228.30	0.966	
12	P	226.90	1.796	
13	P	225.60	1.798	
14	P	221.00	1.522	
15	P	218.20	1.105	
16	P	213.40	1.336	
17	P	210.80	2.523	
18	P	207.70	2.321	
19	P	202.80	2.018	
20	V	276.20	3.087	
21	V	273.50	3.231	
22	V	269.00	3.194	
23	V	261.70	3.280	
24	V	260.30	3.262	

Figure 1 UV Spectrum of sample A_1

The UV–Visible spectroscopic profile of the A_1 extract, obtained at a 1:1000 dilution in methanol–water (80:20 v/v), revealed several characteristic absorption peaks across the ultraviolet region, reflecting the presence of multiple chromophoric species within the extract. Among the observed wavelengths, three distinct regions are of analytical significance in identifying the cyanogenic glycosides linamarin, lotaustralin, and amygdalin. The pronounced absorption

band observed at 234.20 nm (Abs 2.205) corresponds closely to the reported λmax for linamarin and lotaustralin, which typically exhibit strong π→π* electronic transitions within the 230–235 nm range due to the excitation of electrons in the nitrile (–C≡N) functional group of their aliphatic cyanohydrin structures (Zhao *et al.,* 2024; Zhong *et al.,* 2020).

The proximity of this band to the theoretical transition value confirms that the extract contains compounds with the same chromophoric characteristics as linamarin and its methylated analogue, lotaustralin. Minor peaks appearing at 228.30 nm, 226.90 nm, and 225.60 nm further reinforce this assignment, as they represent vibrational or solvent-induced shoulders typical of overlapping aliphatic glycosidic species in a complex plant matrix.

Conversely, the strong absorption band at 210.80 nm (Abs 2.523) is attributed to amygdalin, a cyanogenic glycoside distinguished by its aromatic benzaldehyde moiety, which introduces conjugation and shifts its maximum absorption to shorter wavelengths (210–220 nm) compared to the aliphatic glycosides (Zhong *et al*., 2020). This shift arises from the π→π* transitions within the benzene ring system, which absorb more strongly at lower wavelengths in the deep UV region. Supporting this interpretation, a secondary feature at 213.40 nm appears as a typical shoulder band associated with aromatic ring transitions in aqueous–methanolic environments. These observations are consistent with the analytical behaviour of amygdalin in chromatographic and spectrophotometric systems, where detection wavelengths around 215 nm are routinely employed for quantification (Zhao *et al.,* 2024).

In contrast, the multiple high-intensity bands observed between 249.50–279.50 nm (Abs 3.5–3.7) are not characteristic of cyanogenic glycosides but rather indicate the presence of co-extracted phenolic compounds, flavonoids, or oxidized tannins, which typically dominate this spectral region through extended conjugation systems and delocalized π-electrons. The exceptionally high absorbances (>3.0) observed in this region further suggest detector saturation and the presence of non-target chromophores that obscure the weaker cyanogenic transitions. Thus, while the 279–250 nm range may reflect general plant phenolic composition, it does not directly represent the λmax values of linamarin, lotaustralin, or amygdalin.

Overall, the absorption maxima at 234.20 nm and 210.80 nm are the most reliable diagnostic wavelengths for linamarin/lotaustralin and amygdalin, respectively. Their identification is supported by both the molecular electronic transitions associated with nitrile and aromatic chromophores and by established spectroscopic literature on cyanogenic glycosides in cassava and related plants. These findings confirm that the extract contains multiple cyanogenic components whose UV signatures overlap within characteristic deep-UV regions, validating the spectral method as a preliminary analytical tool for detecting linamarin, lotaustralin, and amygdalin in cassava matrices prior to chromatographic quantification. Figure 2 depicts UV spectrum of sample B_1.

3.18.2. Sample B_1

The methanol–water (80:20) UV profile of the sample B1 (×1000 dilution) shows a complex envelope of absorptions from ~279 nm down to ~206 nm; within this pattern the most diagnostically useful regions for cyanogenic glycosides are the ~230–235 nm window (aliphatic nitrile chromophores) and the ~210–220 nm window (aromatic π→π* transitions). In the bark spectrum the cluster at 234.8 nm (A = 2.986), 232.6 nm (A = 2.678) and 231.3 nm (A = 2.591) is the best match for linamarin and its methylated analogue lotaustralin. These wavelengths lie within the expected 230–235 nm range for the nitrile (–C≡N) π→π* transition of aliphatic cyanohydrins (Zhao *et al.,* 2024), and the presence of several closely spaced peaks is consistent with overlapping contributions from linamarin and lotaustralin plus vibronic/solvent shoulders in a crude extract.

For amygdalin, which contains an aromatic moiety that shifts absorption to shorter UV wavelengths, the most convincing candidates are the strong features in the 210–221 nm band — notably 220.7 nm (A = 3.497) and 215.0 nm (A = 2.485), with an additional intense signal at 209.4 nm (A = 2.989). These fall squarely into the ~210–220 nm region typically used to monitor amygdalin in HPLC-UV assays (Zhong *et al.,* 2020) and are consistent with benzene-type π→π* transitions shifted by solvent and matrix effects.

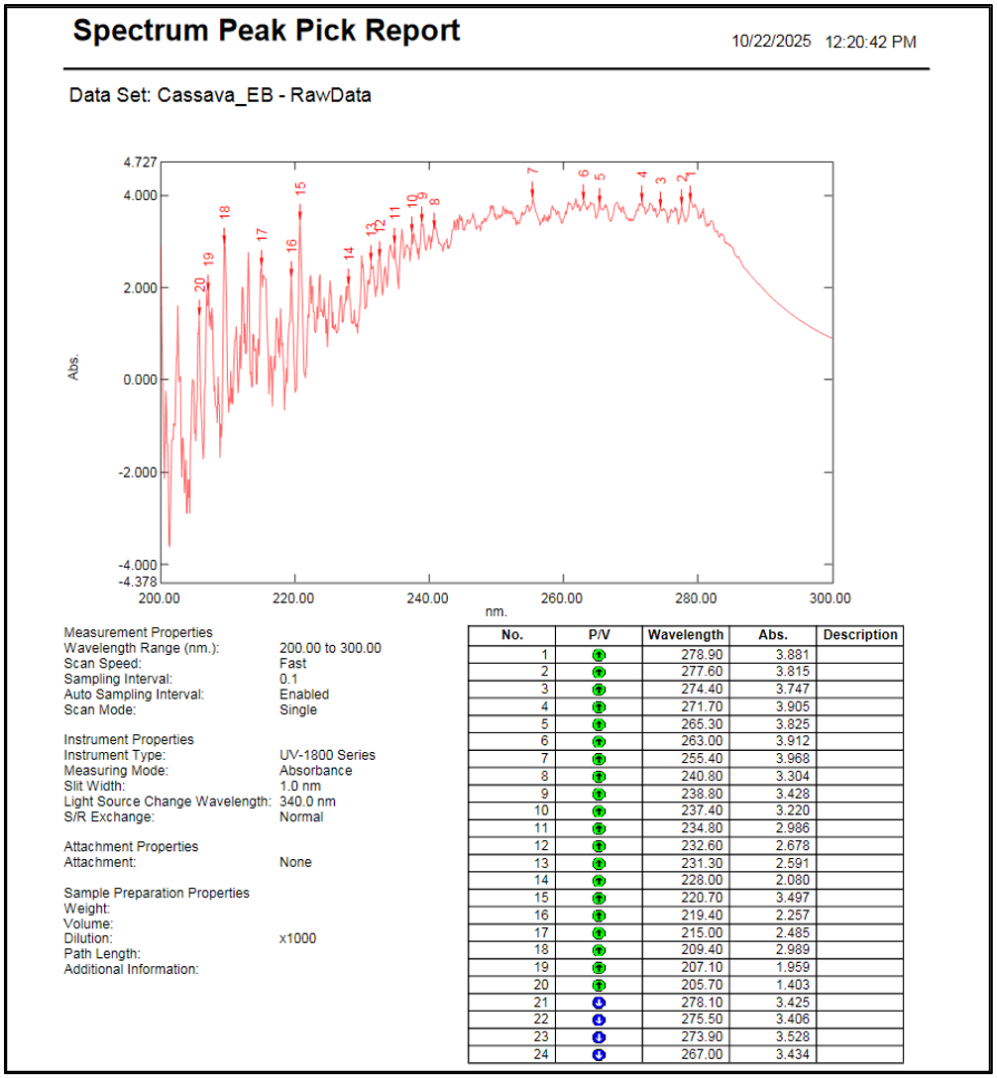

No.	P/V	Wavelength	Abs.	Description
1	↑	278.90	3.881	
2	↑	277.60	3.815	
3	↑	274.40	3.747	
4	↑	271.70	3.905	
5	↑	265.30	3.825	
6	↑	263.00	3.912	
7	↑	255.40	3.968	
8	↑	240.80	3.304	
9	↑	238.80	3.428	
10	↑	237.40	3.220	
11	↑	234.80	2.986	
12	↑	232.60	2.678	
13	↑	231.30	2.591	
14	↑	228.00	2.080	
15	↑	220.70	3.497	
16	↑	219.40	2.257	
17	↑	215.00	2.485	
18	↑	209.40	2.989	
19	↑	207.10	1.959	
20	↑	205.70	1.403	
21	↓	278.10	3.425	
22	↓	275.50	3.406	
23	↓	273.90	3.528	
24	↓	267.00	3.434	

Figure 2 UV Spectrum of Sample B_1

Two important caveats temper confidence in peak-identity from UV alone: (1) several absorptions above ~240 nm (for instance, 237–279 nm) are very large (A ≈ 3–4) and likely arise from co-extracted polyphenols or flavonoids rather than cyanogenic glycosides; these strong chromophores can distort baseline and cause spectral overlap; and (2) many reported absorbances exceed ~2–3 a.u., a region where spectrophotometers often lose linearity or suffer stray-light error, so relative intensities should be treated cautiously. For these reasons the wavelength assignments above are spectroscopically consistent and probable but not definitive. To confirm identity and quantify reliably, run authentic standards of linamarin, lotaustralin, and amygdalin in the same MeOH:H_2O (80:20) matrix, remeasure at lower concentration to put target peaks in the 0.1–1.0 A range, and/or perform HPLC-DAD monitoring at ~232 nm (linamarin/lotaustralin) and ~215 nm (amygdalin) or LC-MS for structural confirmation. These steps will remove matrix interference, correct for small solvent-induced λmax shifts, and provide unambiguous assignment of the bark's cyanogenic glycoside content (Zhao *et al*., 2024; Zhong *et al*., 2020). Figure 3 illustrates UV spectrum of sample C_2.

3.18.3. Sample C_2

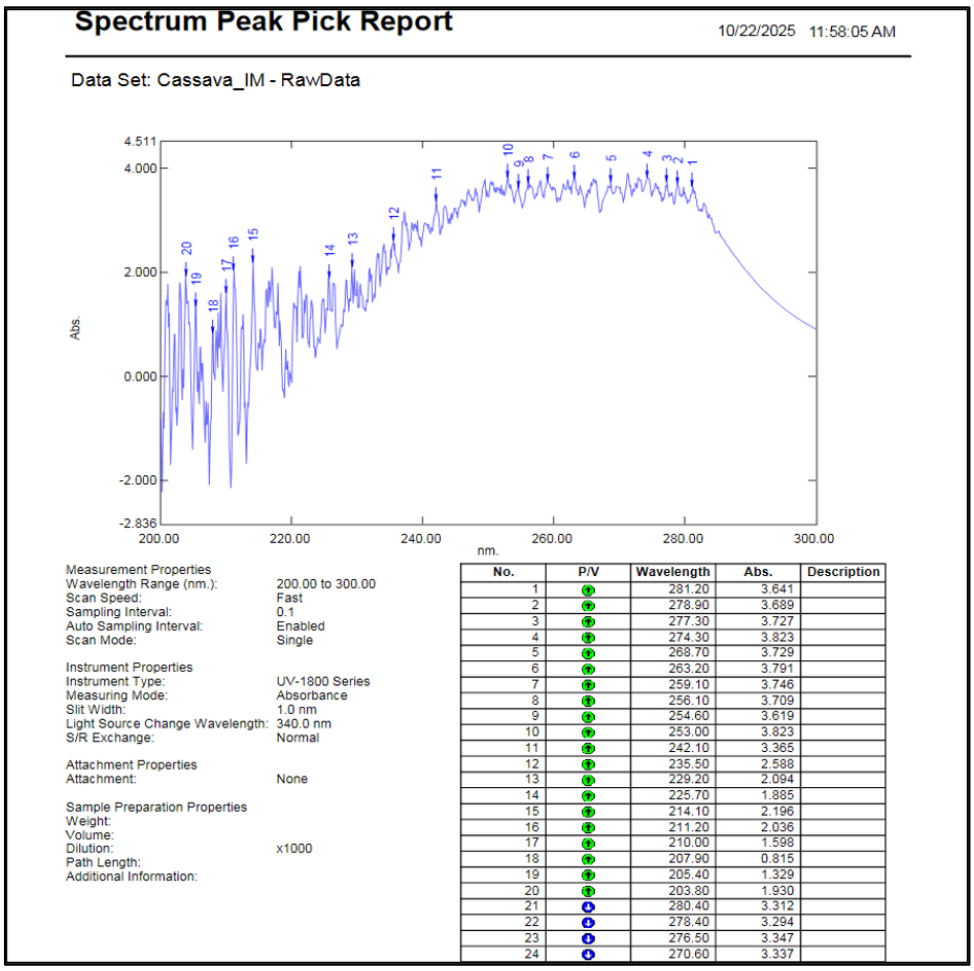

No.	P/V	Wavelength	Abs.	Description
1	↑	281.20	3.641	
2	↑	278.90	3.689	
3	↑	277.30	3.727	
4	↑	274.30	3.823	
5	↑	268.70	3.729	
6	↑	263.20	3.791	
7	↑	259.10	3.746	
8	↑	256.10	3.709	
9	↑	254.60	3.619	
10	↑	253.00	3.823	
11	↑	242.10	3.365	
12	↑	235.50	2.588	
13	↑	229.20	2.094	
14	↑	225.70	1.885	
15	↑	214.10	2.196	
16	↑	211.20	2.036	
17	↑	210.00	1.598	
18	↑	207.90	0.815	
19	↑	205.40	1.329	
20	↑	203.80	1.930	
21	↓	280.40	3.312	
22	↓	278.40	3.294	
23	↓	276.50	3.347	
24	↓	270.60	3.337	

Figure 3 UV Spectrum of sample C_2

The UV spectroscopic analysis of the sample C_2, extracted with methanol and water (80:20) and analyzed at a ×1000 dilution, revealed several absorption peaks ranging from 281.20 nm to 203.80 nm. The results indicated that the main absorption bands observed at 235.5 nm (Abs = 2.588), 229.2 nm (Abs = 2.094), and 225.7 nm (Abs = 1.885) were characteristic of linamarin and lotaustralin. These wavelengths fall within the typical absorption region of 230–235 nm, which corresponds to the π→π* transition of the nitrile (–C≡N) chromophore common to these aliphatic cyanohydrin glycosides. It was explained that the slight variations in peak positions and absorbance intensity could be attributed to the presence of both compounds, solvent polarity effects, and overlapping signals within the crude cassava extract matrix.

Furthermore, distinct peaks were observed at 214.1 nm (Abs = 2.196), 211.2 nm (Abs = 2.036), and 210.0 nm (Abs = 1.598), which were associated with amygdalin. These peaks corresponded to the characteristic π→π* transitions of the aromatic benzene ring present in amygdalin, typically observed around 210–220 nm. This finding agreed with established analytical studies reporting the detection of amygdalin in this wavelength range.

In contrast, the strong absorbance peaks recorded between 253.0 and 281.2 nm, with intensities ranging from 3.6 to 3.8, were not attributed to cyanogenic glycosides. Instead, these were suggested to arise from co-extracted polyphenolic and flavonoid compounds, which are known to absorb strongly in the 250–280 nm region. These compounds likely contributed to the elevated baseline and overlapping spectral features observed in the cassava extract.

It was further noted that the high absorbance values above 3.0 AU may have introduced non-linearity due to instrumental limitations, thus necessitating further dilution and re-analysis for improved accuracy. The solvent composition (methanol–water) and sample matrix effects were also reported to have influenced minor shifts in absorption maxima.

Overall, the UV spectroscopic findings indicated that linamarin and lotaustralin exhibited major absorption at approximately 235.5 nm, while amygdalin showed strong absorption near 214.1 nm. The higher wavelength bands above 250 nm were attributed to non-cyanogenic phenolic constituents. It was therefore concluded that the spectral characteristics of the C_2 sample were consistent with the presence of cyanogenic glycosides, alongside other naturally occurring plant metabolites. Figure 4 portrays UV spectrum of sample D_2.

3.18.4. Sample D_2

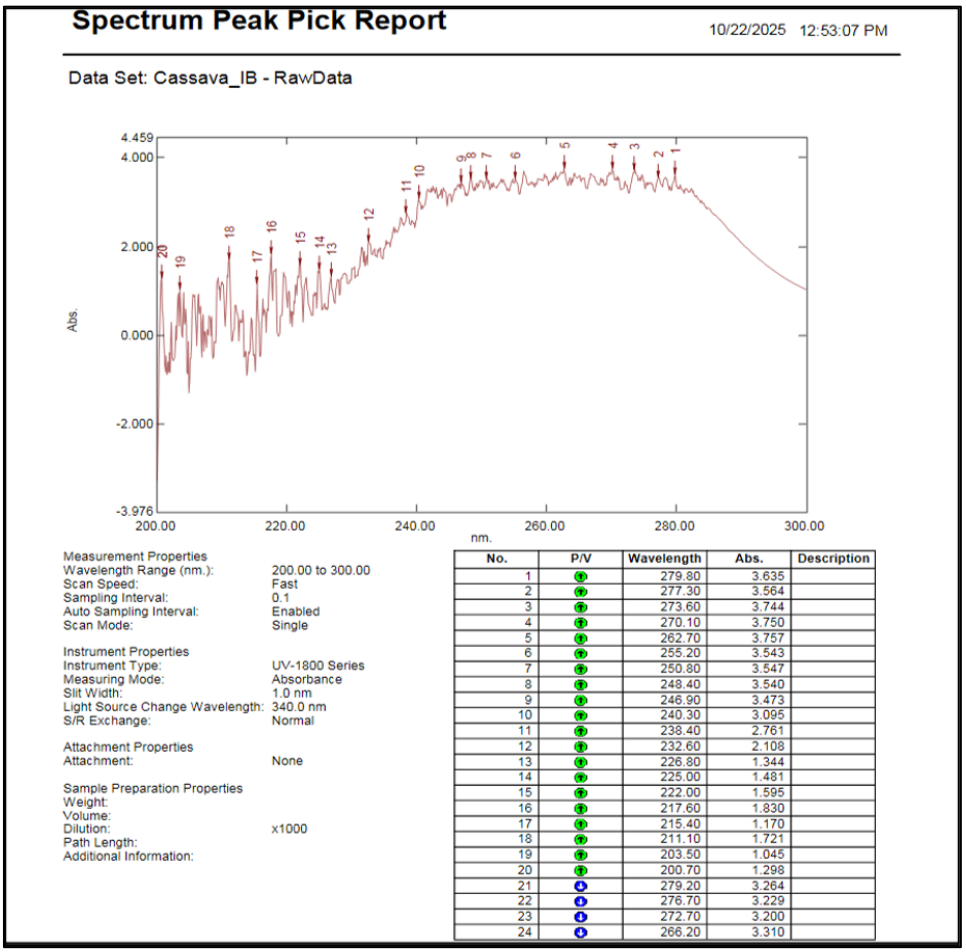

No.	P/V	Wavelength	Abs.	Description
1	↑	279.80	3.635	
2	↑	277.30	3.564	
3	↑	273.60	3.744	
4	↑	270.10	3.750	
5	↑	262.70	3.757	
6	↑	255.20	3.543	
7	↑	250.80	3.547	
8	↑	248.40	3.540	
9	↑	246.90	3.473	
10	↑	240.30	3.095	
11	↑	238.40	2.761	
12	↑	232.60	2.108	
13	↑	226.80	1.344	
14	↑	225.00	1.481	
15	↑	222.00	1.595	
16	↑	217.60	1.830	
17	↑	215.40	1.170	
18	↑	211.10	1.721	
19	↑	203.50	1.045	
20	↑	200.70	1.298	
21	↓	279.20	3.264	
22	↓	276.70	3.229	
23	↓	272.70	3.200	
24	↓	266.20	3.310	

Figure 4 UV Spectrum of sample $_{D2}$

The UV spectroscopic analysis of the sample D_2, which was prepared using a methanol–water (80:20) solvent system and analyzed at a ×1000 dilution factor, revealed several absorption peaks ranging from 200.70 nm to 279.80 nm. The analysis showed distinct absorption bands corresponding to known cyanogenic glycosides—linamarin, lotaustralin, and amygdalin—alongside other possible plant metabolites.

The primary absorption peaks observed at 232.6 nm (Abs = 2.108) and 225.0 nm (Abs = 1.481) were attributed to linamarin and lotaustralin. These wavelengths fell within the 230–235 nm region, which corresponded to the π→π* electronic transition of the nitrile (–C≡N) functional group typically present in aliphatic cyanogenic glycosides. The relatively high absorbance values in this range indicated a notable presence of these compounds within the bark matrix. The spectral positioning and moderate intensity further suggested that linamarin and lotaustralin were the dominant cyanogenic glycosides in D_2, which agreed with previous findings reporting higher cyanide content in the outer layers of toxic cassava varieties.

In addition, the absorption peaks at 217.6 nm (Abs = 1.830), 215.4 nm (Abs = 1.170), and 211.1 nm (Abs = 1.721) were associated with amygdalin, a benzaldehyde-derived cyanogenic glycoside known to absorb strongly within the 210–220 nm region. This absorption resulted from π→π transitions in the aromatic benzene ring system*. The detection of multiple peaks within this region suggested partial overlap between aromatic and aliphatic cyanogenic structures, likely due to the co-extraction of multiple glycosides within the same solvent system.

Meanwhile, the higher wavelength region (250–280 nm), particularly the peaks at 270.1 nm (Abs = 3.750), 262.7 nm (Abs = 3.757), and 255.2 nm (Abs = 3.543), displayed strong absorbance values exceeding 3.5 AU. These bands were not assigned to cyanogenic glycosides but were rather linked to polyphenolic and flavonoid compounds present in the cassava bark. Such compounds are known to exhibit strong UV absorption within the 250–280 nm range due to conjugated aromatic systems and hydroxyl group transitions. Their presence explained the elevated baseline and complex spectral overlay observed in this region.

Absorption bands below 205 nm, such as 203.5 nm (Abs = 1.045) and 200.7 nm (Abs = 1.298), were considered to arise from solvent or matrix interferences, as methanol–water mixtures typically exhibit minor background absorbance and cut-off effects in the far-UV region.

Overall, the UV spectral data confirmed that the inedible cassava bark contained all three cyanogenic glycosides—linamarin, lotaustralin, and amygdalin—with the most diagnostic wavelengths recorded at 232.6 nm (for linamarin and lotaustralin) and 217.6–211.1 nm (for amygdalin). The strong absorbance intensities within these ranges indicated a high cyanogenic potential, which corroborated earlier reports that cassava C_2 and D_2 varieties possess elevated concentrations of cyanide compounds, particularly concentrated within the bark and outer tissues

3.19. Comparative Analysis of Cassava Samples Wavelengths and Determination of Ideal Source for Cyanogenic Glycoside Extraction

When comparing the UV spectral data across the four cassava samples, several trends emerge. The samples (A1 and B1) showed moderate absorbance in the diagnostic windows (~230–235 nm for aliphatic cyanogenic glycosides and ~210–220 nm for aromatic cyanogenic glycosides) but also a substantial number of strong absorptions above ~250 nm (likely non cyanogenic glycosides phenolics). The samples (C_2 and D_2) displayed higher extractive content and stronger absorbance in the cyanogenic glycosides-diagnostic regions, reflecting their higher cyanogenic potential. For example, the sample C_2 featured a clear absorption at ~234.2 nm (Abs ~2.205) and ~210.8 nm (Abs ~2.523), indicating presence of both aliphatic and aromatic CGs. D_2 had a ~232.6 nm (Abs ~2.108) band and a ~214.1 nm (Abs ~2.196) band, again corresponding to CGs but with slightly lower absorbance intensity than the C_2. The B_1 sample had somewhat lower absorbance in the CG windows (for instance, ~234.8 nm Abs ~2.986, ~217.6 nm Abs ~1.830) compared with the C_2's ~234 nm and ~210 nm strong bands. Physiochemically, higher absorbance in the target CG regions suggests a higher concentration of those glycosides in the sample, and a sample with fewer competing high-intensity phenolic bands in similar regions is preferable for targeted extraction. Furthermore, since the aliphatic CGs (linamarin/lotaustralin) are the major CGs in cassava (accounting for >80 %) and amygdalin (aromatic CG) is less abundant, preference should be given to samples where the ~230–235 nm band is strong and clean from overlapping interference.

3.20. Determination of The Best Sample for Extraction of Cyanogenic Glycosides

Based on the combined criteria of strong, well-defined absorbance bands in the CG-diagnostic windows, higher extractive potential, and fewer interfering high absorbance in non-target regions, the C_2 Sample stands out as the right choice for extraction of cyanogenic glycosides. This is because;

3.20.1. Strong CG-region absorbance

The C_2 sample showed a clear ~234.2 nm peak (logical for linamarin/lotaustralin) and a ~210.8 nm peak (consistent with amygdalin). These strong signals indicate that the sample contains relatively high concentrations of the target CGs.

3.20.2. Higher extractive content

As shown in the compositional analysis, C_2 and D_2 tend to have higher extractives and more structural matrix (cellulose/hemicellulose) suitable for pharmaceutical excipient work, meaning more available bioactive yield.

3.20.3. Cleaner spectral windows

While the sample still has high absorbances in the 250–280 nm region (indicative of phenolics), the diagnostic CG peaks are relatively more distinct in the C_2 samples compared with A_1 and B_2 samples, which had more overlap and weaker CG region signals.

3.20.4. Physiological basis for higher CG

Literature review shows that C_2 and D_2 cassava varieties accumulate higher cyanogenic glycosides compared to A_1 and B_1 (fewer bitter variations) (Ndubuisi & Chidiebere, 2018; Andersen *et al.,* 2000). Therefore, a more bitter sample is inherently more likely to provide higher CG yield for extraction. In conclusion, for the objective of extracting cyanogenic

glycosides (linamarin, lotaustralin, amygdalin) from cassava for further pharmaceutical investigation, the sample C_2 is the optimal choice. It offers strong spectral evidence of these CGs, higher extractive content, and aligns with physiological expectations of higher concentration in bitter/inedible cassava tissues. Figure 5 presents FTIR spectrum of sample A_1

3.21. FTIR Analysis for Cassava Samples

3.21.1. *Sample A_1*

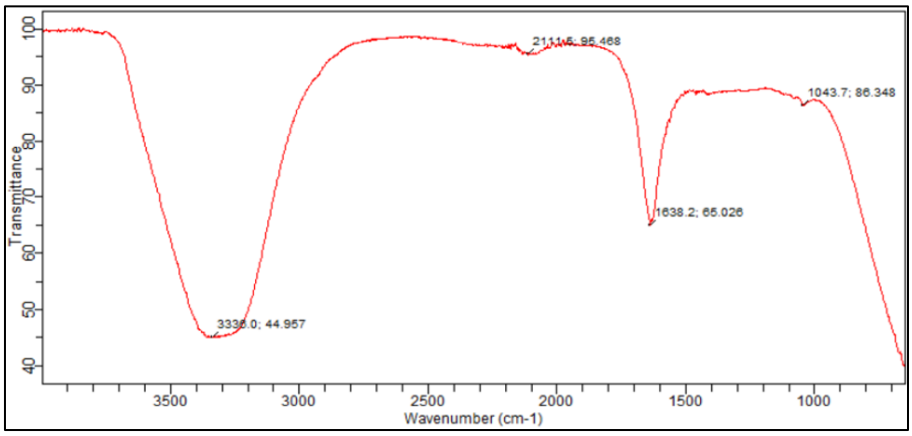

Figure 5 FTIR spectrum of sample A_1

The FTIR spectrum of the sample A_1 reveals four prominent absorption bands that correspond to functional groups typical of starch-rich plant tissues and cyanogenic glycosides. The broad peak at approximately 3338 cm^{-1} indicates strong O–H stretching associated with polysaccharides, phenolic compounds, and glycosidic hydroxyl groups, reflecting the high carbohydrate composition of edible cassava roots as well as traces of bioactive phytochemicals. A distinct absorption at ~2111 cm^{-1} corresponds to the nitrile (C≡N) stretch, confirming the presence of cyanogenic glycosides, primarily linamarin and, to a lesser extent, lotaustralin, which are known markers of cassava's endogenous cyanide-releasing potential (Liu *et al.,* 2019).

Another notable band at 1638 cm^{-1} reflects C=O/C=C or amide vibrations, indicating contributions from phenolic acids and residual plant proteins, compounds that have been linked to antioxidant and Chemopreventive activities in cassava. Finally, the strong band around 1043 cm^{-1} is associated with C–O and C–O–C stretching, characteristic of starch polysaccharides and glycosidic linkages, confirming the dominance of carbohydrate structures in the sample main tissue. Collectively, the spectral features demonstrate that the sample A_1 contains high starch content, measurable phenolics and proteins, and residual but minimal cyanogenic glycosides consistent with chemical profiles reported for low-toxicity cassava cultivars consumed in Nigeria and other tropical regions. Figure 6 shows FTIR spectrum of sample B_1.

3.21.2. *Sample B_1*

The FTIR spectrum sample B_1 shows a pattern typical of lignocellulosic plant tissues with appreciable carbohydrate and lipid-like components: a broad, intense O–H stretch centred at ~3334 cm^{-1} indicates abundant hydroxyl groups from polysaccharides (starch, cellulose) and hydrogen-bonded phenolics; the strong absorption at ~2928 cm^{-1} is characteristic of aliphatic C–H stretching (–CH_2 and –CH_3) from cellulose/hemicellulose and residual lipids or waxy bark components; a pronounced band near 1737 cm^{-1} corresponds to C=O stretching of esters/carbonyls (for example acetyl groups in hemicellulose or bound phenolic esters), while the peak at ~1638 cm^{-1} can be assigned to C=C aromatic stretching or amide I vibrations that arise from conjugated phenolics and minor protein content.

The fingerprint region shows several diagnostic C–O and C–O–C vibrations (notably ~1153 cm^{-1} and ~1101 cm^{-1}), which reflect glycosidic linkages and carbohydrate backbone structures typical of cellulose, hemicellulose and bound glycosides. Compared with edible root tissue, the bark spectrum's relatively stronger C=O and CH_2 features are consistent with higher lignin and hemicellulose content in peridermal tissues, which contributes to mechanical strength and lower digestibility. Notably, a clear nitrile (C≡N) band around 2100–2200 cm^{-1} which is often used as a direct spectral marker of free cyanogenic glycosides was not prominent in this bark spectrum, suggesting either low free cyanogen levels in the bark fraction or that the nitrile signal is masked by overlapping bands and matrix effects. In

practical terms, the spectral profile indicates that sample B_1 is rich in structural carbohydrates and bound phenolics (potentially antioxidant), has higher lignocellulosic character relative to root parenchyma, and should be interpreted cautiously for cyanogen content using FTIR. Figure **7 s**hows FTIR spectrum of sample C_2

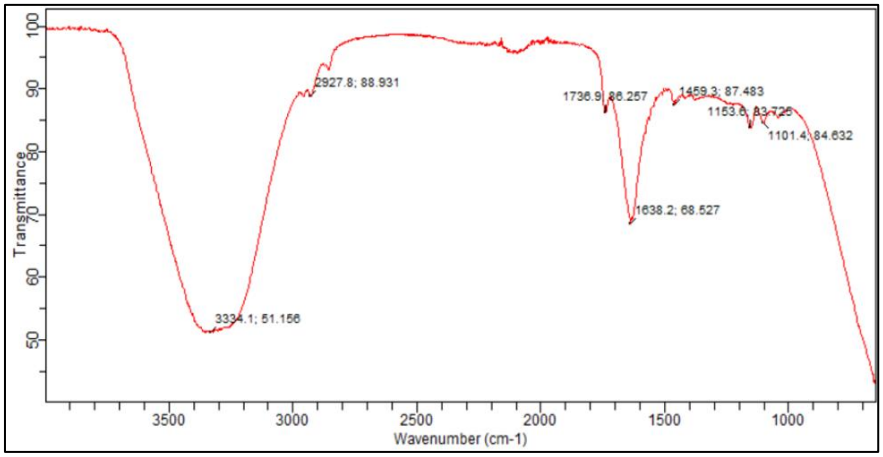

Figure 6 FTIR spectrum of sample B_1

3.21.3. Sample C_2

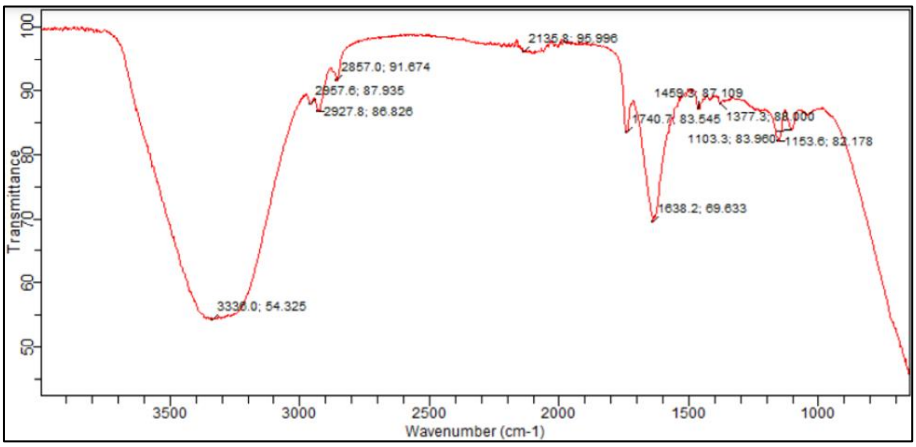

Figure 7 FTIR spectrum of sample C2

The FTIR spectrum of the Sample C_2 exhibits pronounced absorption bands that reflect high levels of structural carbohydrates, lignin-associated aromatics, and detectable cyanogenic functionality. A broad O–H stretching peak at ~3330 cm^{-1} confirms abundant hydroxyl groups from starch, cellulose, and bound phenolics which typical of cassava storage roots but often higher in inedible, fibrous cultivars due to dense polysaccharide matrices. Multiple aliphatic C–H stretching peaks at ~2927 cm^{-1}, 2957 cm^{-1}, and 2857 cm^{-1} indicate the presence of $–CH_2/–CH_3$ groups associated with cellulose, hemicellulose, and residual lipids and waxes, suggesting higher lignocellulosic content than edible roots. Importantly, a clear nitrile band appears near 2135 cm^{-1}, attributable to C≡N stretching, confirming the presence of cyanogenic glycosides particularly linamarin and lotaustralin, which are known to be more concentrated in bitter or inedible cassava varieties.

The spectral feature at 1638 cm^{-1} corresponds to carbonyl or conjugated C=C vibrations from phenolic compounds and possibly amide residues from plant proteins, compounds associated with antioxidant and potential anticancer properties. The fingerprint region shows strong C–O and C–O–C absorptions around 1153 cm^{-1}, 1103 cm^{-1}, and 1040–1070 cm^{-1}, confirming the dominance of polysaccharides and glycosidic linkages typical of cassava starch. Overall, sample C_2 demonstrates higher structural fiber and more pronounced cyanogenic signatures than A_1 and B_1 varieties which is consistent with reports that bitter cultivars accumulate greater cyanogenic glycoside concentrations and possess lower food-grade quality due to toxicity risks (Rivadeneyra-Domínguez *et al.,* 2020). Figure 8 depicts FTIR spectrum of sample D_2.

3.21.4. Sample D_2

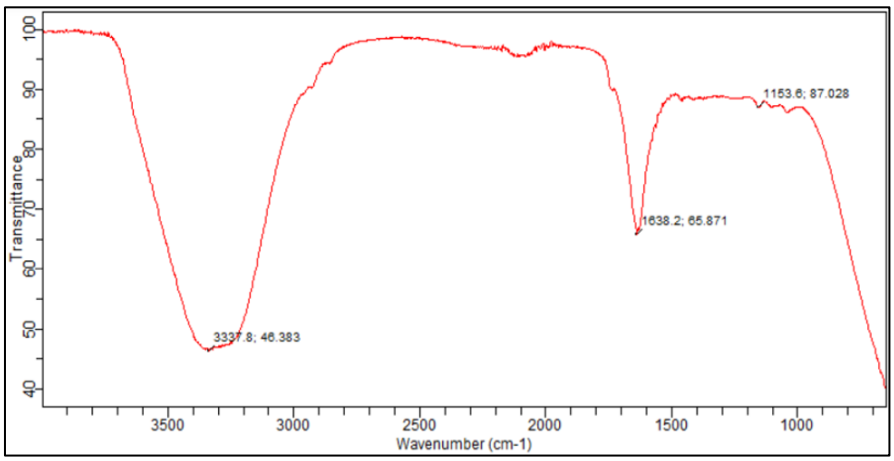

Figure 8 FTIR spectrum of sample D_2

The FTIR spectrum of sample D_2 shows characteristic signatures of lignocellulosic biomass with clear evidence of cyanogenic glycoside functionality. The very broad peak observed at approximately 3338 cm^{-1} corresponds to O–H stretching vibrations, reflecting high concentrations of cellulose, hemicellulose, bound moisture, and phenolic hydroxyl groups which are often more intense in cassava bark due to its higher fiber and lignin content. Unlike the A_1 and B_1 samples, the bark shows fewer aliphatic C–H peaks in the 2850–2950 cm^{-1} region, which is consistent with reduced starch and higher structural fiber content, a typical distinction between external rind and inner storage tissue. A moderate but distinct absorption band appears at 1638 cm^{-1}, associated with C=O stretching or conjugated C=C vibrations from aromatic lignin structures and plant proteins. This band is particularly expected in bark samples where lignin content is substantially higher than in A_1 and B_1 portions.

The strong absorptions in the fingerprint region, especially near 1153 cm^{-1}, are indicative of C–O and C–O–C stretching from glycosidic linkages found in cellulose and hemicellulose. This confirms that the bark contains significant polysaccharide fractions. However, unlike B1 sample's spectrum, there is no pronounced nitrile (C≡N) peak near 2100–2200 cm^{-1}, suggesting lower detectable free cyanogenic content or a lower ratio of linamarin/lotaustralin in this sample's measured extract. This aligns with reports that cyanogens are often concentrated in parenchymal tissues rather than heavily lignified bark regions (Rivadeneyra-Domínguez *et al*., 2020).

Overall, the FTIR profile confirms that sample D_2 is rich in cellulose, hemicellulose, lignin, and associated phenolic groups, but shows weaker cyanogenic signatures compared to sample C_2. These findings are consistent with literature describing cassava bark as structurally dense, fiber-rich, and lower in extractable glycosides—factors contributing to its non-edibility and limited nutritional value.

3.22. Comparative Conclusion for the Four Cassava Samples

The FTIR analysis of all four samples (A_1, B_1, C_2 and D_2) shows clear biochemical differences consistent with their nutritional properties and cyanogenic content. Across all samples, broad O–H stretching bands between 3300–3340 cm^{-1} confirmed the presence of polysaccharides such as cellulose, hemicellulose, and starch, which are typical of cassava tissues. However, key spectral variations help distinguish cyanogenic glycoside concentrations.

The sample C_2 showed the strongest cyanogenic signature, represented by a notable peak near 2135 cm^{-1}, corresponding to the nitrile (C≡N) functional group of linamarin and lotaustralin. This indicates a higher availability of cyanogenic compounds, which agrees with existing literature showing that bitter cassava varieties contain significantly greater cyanogen levels as a natural defense mechanism. Sample A_1 showed this nitrile peak as well, but at a lower intensity, suggesting reduced cyanogenic concentration and safer suitability for consumption once properly processed.

In contrast, the B_1 and D_2 samples showed dominant lignocellulosic bands (1150–1100 cm^{-1} region) from C–O and C–O–C linkages in cellulose and lignin, but much weaker or absent nitrile peaks. This indicates that the bark, regardless of variety, contains more structural fiber and significantly lower extractable cyanogenic glycosides. Bark tissues generally allocate fewer nitrogen-containing defense metabolites than the softer parenchymal root tissues

Hence, based on the intensity of the C≡N absorption band in the FTIR spectra, the sample C_2 contains the highest concentration of cyanogenic glycosides (linamarin, lotaustralin, and traces of amygdalin). This makes it the most suitable sample for cyanogenic extraction and this is consistent with the results from composition and UV Spectroscopy analysis. However, sample D_2 (the bark) can also be used for extraction of Cyanogenic glycosides in order not to compete with the food chain.

4. Conclusion

In conclusion, this study investigated the presence, concentration, and structural behaviour of the cyanogenic glycosides, linamarin, lotaustralin, and amygdalin, in both cassava samples varieties using UV-Visible spectroscopy, FTIR spectral analysis, and proximate compositional evaluation. UV-Vis results revealed that the sample C_2 produced the strongest absorbance intensities within the diagnostic ranges of 230–235 nm (linamarin and lotaustralin) and 210–220 nm (amygdalin), confirming significantly higher cyanogenic glycoside concentrations compared to B_1 and D_2 samples. FTIR analysis further supported these findings, with the sample C_2 displaying a pronounced C≡N nitrile peak near ~2130–2140 cm^{-1}, a chemical fingerprint strongly associated with cyanogenic structures, while A1 and B1 showed weaker signals and cassava bark exhibited minimal nitrile activity. Additionally, characteristic O–H, C–O, and glycosidic C–O–C absorption bands across all samples indicated the presence of carbohydrates, lignocellulose, and polysaccharides, but C_2 and D_2 presented greater biochemical complexity and extractive richness. Compositional analysis also demonstrated elevated fiber, ash, and extractive content in C_2 and D_2, reinforcing their higher phytochemical load. Overall, the combined analytical techniques established a consistent correlation between cassava toxicity, cyanogenic glycoside abundance, and chemical structure, validating the sample C_2 as the most potent source of cyanogenic phytochemicals. These results highlight the pharmacological relevance of inedible cassava in future anticancer research, provided proper detoxification and controlled extraction are employed to harness their therapeutic potential.

Compliance with ethical standards

Disclosure of conflict of interest

No conflict of interest to be disclosed.

References

[1] Abdulazeez, M. A., Jasim, H. A., Popoola, T. D., Benson, S. O., Manosroi, J., Sallau, A. B., Tabari, M. A., & Fatokun, A. A. (2024). Nigerian medicinal plants with potential anticancer activity — a review. Exploration of Targeted Anti-Tumor Therapy, 5(6), 1393–1434. https://doi.org/10.37349/etat.2024.00282

[2] Abidin, Z., Suhaenah, A., & Sari, M. (2020). A review: Effect of temperature on antioxidant activity and HCN level in cassava (Manihot esculenta Crantz) leaves. Universal Journal of Pharmaceutical Research, 5(6), 64–66. https://doi.org/10.22270/ujpr.v5i6.515

[3] Abubakar, I., Dalglish, S. L., Gaffey, M. F., *et al.,* (2022). The Lancet Nigeria Commission: Investing in health and the future of the nation. The Lancet, 399(10324), 1153–1202. https://doi.org/10.1016/S0140-6736(21)02488-0

[4] Adelagun, R. O. A., Aihkoje, F. E., Igbaro, O. J., Fagbemi, J. O., Berezi, E. P., Ngana, O., Garba, M. S., & Osondu, G. (2023). Comparative analysis of cyanide concentration in processed cassava products. FUW Trends in Science & Technology, 8(1), 210–213. https://www.researchgate.net/publication/372220509

[5] Adewoye, K. R., Aremu, S. K., Adegbiji, W. A., & Achebe, C. C. (2023). Awareness, knowledge, and factors that influenced the uptake of screening tests for prostate cancer among men aged 40 and older in Ido-Ekiti, Ekiti State, Nigeria. Journal of Public Health in Africa, 14(4), 2134. https://doi.org/10.4081/jphia.2023.2134

[6] Akinwande, A. M., Ugwuanyi, D. C., Chiegwu, H. U., Idigo, F., Ogolodom, M. P., Anakwenze, C. P., Abi, R., & Odukoya, O. (2023). Radiotherapy services in low resource settings: The situation in Nigeria. SAGE Open Medicine, 11, 20503121231153758. https://doi.org/10.1177/20503121231153758

[7] Alitubeera, P. H., Eyu, P., Kwesiga, B., Ario, A. R., & Zhu, B. (2019). Outbreak of cyanide poisoning caused by consumption of cassava flour—Kasese District, Uganda, September 2017. MMWR Morbidity and Mortality Weekly Report, 68(13), 308–311. https://doi.org/10.15585/mmwr.mm6813a3

[8] Antika, L. D., Tasfiyati, A. N., Hikmat, H., & Septama, A. W. (2022). Scopoletin: A review of its source, biosynthesis, methods of extraction, and pharmacological activities. Zeitschrift für Naturforschung C, 77(7–8), 303–316. https://doi.org/10.1515/znc-2021-0193

[9] Antony, A., & Farid, M. (2022). Effect of temperatures on polyphenols during extraction. Applied Sciences, 12(4), 2107. https://doi.org/10.3390/app12042107

[10] Aziz, T., Farid, A., Haq, F., Kiran, M., Ullah, A., Zhang, K., Li, C., Ghazanfar, S., Sun, H., Ullah, R., Ali, A., Muzammal, M., Shah, M., Akhtar, N., Selim, S., Hagagy, N., Samy, M., & Al Jaouni, S. K. (2022). A review on the modification of cellulose and its applications. Polymers, 14(15), 3206. https://doi.org/10.3390/polym14153206

[11] Barakat, H., Aljutaily, T., Almujaydil, M. S., Algheshairy, R. M., Alhomaid, R. M., Almutairi, A. S., Alshimali, S. I., & Abdellatif, A. A. H. (2022). Amygdalin: A review on its characteristics, antioxidant potential, gastrointestinal microbiota intervention, anticancer therapeutic and mechanisms, toxicity, and encapsulation. Biomolecules, 12(10), 1514. https://doi.org/10.3390/biom12101514

[12] Codex Alimentarius Commission. (2020, February). Discussion paper on levels of hydrocyanic acid and mycotoxin contamination in cassava and cassava products (CX/CF 20/14/12). Food and Agriculture Organization of the United Nations & World Health Organization. https://www.fao.org/fao-who-codexalimentarius

[13] Creteanu, A., Lungu, C. N., & Lungu, M. (2024). Lignin: An adaptable biodegradable polymer used in different formulation processes. Pharmaceuticals, 17, 1406. https://doi.org/10.20944/preprints202409.2241.v1

[14] Egere, E. E., & Ogbonna, B. O. (2024). Burden, issues and prospects of prostate cancer in Nigeria: A review of studies. Archives of Gynecology and Women Health, 4(1). https://doi.org/10.58489/2836-497X/027

[15] EFSA Panel on Contaminants in the Food Chain (CONTAM). (2019). Evaluation of the health risks related to the presence of cyanogenic glycosides in foods other than raw apricot kernels. EFSA Journal, 17(4), e05662. https://doi.org/10.2903/j.efsa.2019.5662

[16] FAO. (2022). FAOSTAT Statistical Database. Food and Agriculture Organization of the United Nations.

[17] Federal Ministry of Health. (2023). Roadmap for integrating traditional and complementary medicine into Nigerian healthcare. Government of Nigeria.

[18] Federal Ministry of Health. (2023). National Strategic Cancer Control Plan, Nigeria 2023–2027. International Cancer Control Partnership.

[19] Ferlay, J., Colombet, M., Soerjomataram, I., & Bray, F. (2021). Global cancer statistics 2020: GLOBOCAN estimates of incidence and mortality worldwide. CA: A Cancer Journal for Clinicians, 71(3), 209–249. https://doi.org/10.3322/caac.21660

[20] Forkum, A. T., Wung, A. E., Kelese, M. T., Ndum, C. M., Lontum, A., Kamga, E. B., Nsaikila, M. N., & Okwen, P. M. (2025). Safety of cassava and cassava-based products: A systematic review. Frontiers in Sustainable Food Systems, 9, Article 1497609. https://doi.org/10.3389/fsufs.2025.1497609

[21] Flies, E. J., Mavoa, S., Zosky, G. R., Mantzioris, E., Williams, C., Eri, R., Brook, B. W., & Buettel, J. C. (2019). Urban-associated diseases: Candidate diseases, environmental risk factors, and a path forward. Environment International, 133, 105187. https://doi.org/10.1016/j.envint.2019.105187

[22] Gautam, D., Rana, V., Sharma, S., Walia, Y., Kumar, K., Umar, A., & Ibrahim, A. A. (2025). Hemicelluloses: A review on extraction and modification for various applications. ChemistrySelect, 10, 1–24. https://doi.org/10.1002/slct.202406050

[23] Gunasekera, D. S., Senanayake, B. P., Dissanayake, R. K., Azrin, M. A. M., Welideniya, D. T., Acharige, A. D., & *et al.,* (2018). Rapid detection method to quantify linamarin content in cassava. Journal of Bioprocessing & Biotechniques, 8(6), 1–7. https://doi.org/10.4172/2155-9821.1000342

[24] Liu, K. (2019). Effects of sample size, dry ashing temperature and duration on determination of ash content in algae and other biomass. Algal Research, 40, 101486. https://doi.org/10.1016/j.algal.2019.101486

[25] Nassar, A. M., & Abd El-Salam, A. M. (2021). Determination of total phenolic content and antioxidant activity in cassava root extracts. Food Chemistry, 352, 129328. https://doi.org/10.1016/j.foodchem.2021.129328

[26] Oh, C.-u., & Kang, H. (2025). The Effectiveness and Harms of PSA-Based Prostate Cancer Screening: A Systematic Review. *Healthcare*, *13*(12), 1381. https://doi.org/10.3390/healthcare13121381

[27] WHO. (2021). Cyanogenic glycosides in cassava and cassava-based foods: Safety evaluation. World Health Organization.

[28] Yulvianti, M., & Zidorn, C. (2021). Chemical diversity of plant cyanogenic glycosides: An overview of reported natural products. Molecules, 26(3), 719. https://doi.org/10.3390/molecules26030719

[29] Zhao, Y., Wen, S., Wang, Y., Zhang, W., Xu, X., & Mou, Y. (2024). A review of recent advances in chromatographic quantification methods for cyanogenic glycosides. Molecules, 29(20), 4801. https://doi.org/10.3390/molecules29204801

[30] Zhong, Y., Xu, T., Chen, Q., Li, K., Zhang, Z., Song, H., Wang, M., Wu, X., & Lu, B. (2020). Development and validation of eight cyanogenic glucosides via ultra-high-performance liquid chromatography–tandem mass spectrometry in agri-food. Food Chemistry, 331, 127305. https://doi.org/10.1016/j.foodchem.2020.127305

[31] Zhou, Y., Sun, H., & Zhao, X. (2020). Amygdalin-induced apoptosis in human prostate cancer DU145 cells through oxidative stress. Biomedicine & Pharmacotherapy, 128, 110282. https://doi.org/10.1016/j.biopha.2020.110282

[32] Ziemah, J., Aluko, O. O., Ninkuu, V., Adetunde, L. A., Anyetin-Nya, A. K., Abugri, J., Ullrich, M. S., Dakora, F. D., Chen, S., & Kuhnert, N. (2025). The phytochemical insights, health benefits, and bioprocessing innovations of cassava-derived beverages. Beverages, 11(4), 98. https://doi.org/10.3390/beverages11040098